Author(s): G. Gregori and D. O. Gericke
Article Title: Low frequency structural dynamics of warm dense matter

Year of publication: 2009
Link to published version:
http://dx.doi.org/ 10.1063/1.3100203
Publisher statement: None

G. Gregori and D.O. Gericke, Physics of Plasmas **16**, 056306 (2009)

Low frequency structural dynamics of warm dense matter

G. Gregori

Clarendon Laboratory, Department of Physics,

University of Oxford, Oxford OX1 3PU, UK

D. O. Gericke

Centre for Fusion, Space and Astrophysics, Department of Physics,

University of Warwick, Coventry CV4 7AL, UK

Abstract

Measurements of the microscopic response of warm dense matter have been demonstrated by multi-keV inelastic x-ray scattering using laser-based sources. These techniques have been used to study the high frequency electron correlations (plasmons) in low to mid-Z plasmas. The advent of 4^{th} generation light sources will provided high fluxes of narrowband and coherent x-rays that will allow to look at the low frequency correlations (the ion-acoustic waves). In this paper we present an analysis of such low frequency modes by calculating the frequency dependent ion-ion structure factor. Our model includes all the relevant multi-body contributions arising from strong coupling and non ideal plasma effects. In particular, the ion-ion structure factor is obtained within the memory function formalism by satisfying a finite number of the sum rules. This work could be used as a basis to a direct experimental test of dense plasma model as soon as keV free electron laser sources will become available.

I. INTRODUCTION

The warm dense matter (WDM) regime, defined by temperatures of a few electron volts and densities comparable with solids, is a complex state of matter where multi-body particle correlations and quantum effects play an important role in determining the overall structure and equation of state [1, 2]. The study of WDM states has practical applications for controlled thermonuclear fusion [3], and it also represents laboratory analogues of astrophysical environments found in the core of planets and the crusts of old stars [4].

The experimental characterisation and theoretical modelling of warm dense matter pose severe challenges since WDM spans the intermediate states between solids and plasmas and retains properties common to both. It exhibits moderately-to-strongly coupled, but fluid-like ions that prohibit the exploitation of long range order as in solids. Expansion techniques used in plasma physics that incorporate correlations perturbatively are also not applicable. From an experimental point of view, the high densities of free electrons make WDM opaque in the visible and, therefore, usual spectroscopic techniques are not possible. To overcome these limitations, x-ray and proton radiography have been applied to obtain density profiles [5, 6]. In the recent years x-ray scattering has gained considerable attention as an alternative diagnostic method in both isochorically heated and shock compressed matter [7–11].

The experimentally measured x-ray scattering cross section contains information about the microscopic structure of the material since it is directly proportional to the total dynamic structure factor of the scattering electrons:

$$\frac{d^2\sigma}{d\Omega d\omega} \propto S_{ee}^{tot}(k,\omega)\,. \tag{1}$$

Here, $k = |\mathbf{k}_0 - \mathbf{k}_1| = (4\pi/\lambda_0)\sin(\Theta/2)$ is the momentum transfer to the photon, $\mathbf{k}_0$ and $\mathbf{k}_1$ are the wave numbers of the incident and the scattered photon, respectively, λ_0 is the wavelength of the incident x-rays, and Θ is the scattering angle; $\omega = \omega_0 - \omega_1$ is the related energy transfer to or from the photon. On average, the photon energy loss is given by the Compton formula $E_C = \hbar^2 k^2/2m_e$.

The dynamic structure factor $S_{ee}^{tot}(k,\omega)$ is a measure for the spatial correlations in the system (unity for uncorrelated systems). The long range nature of the Coulomb interactions that govern the WDM state gives rise to collective excitations, namely the ion acoustic and the electron plasma modes. These become particularly important in the long wavelength

limit (*i.e.*, $k \to 0$), and result in peaks in the structure factor. $S_{ee}^{tot}(k,\omega)$ can be decomposed into three parts that highlight both modes plus an additional term that includes resonant processes [12, 13]

$$S_{ee}^{tot}(k,\omega) = |f_I(k) + q(k)|^2 S_{ii}(k,\omega) + ZS_{ee}^0(k,\omega) + Z_c \int \tilde{S}_{ce}(k,\omega-\omega')S_s(k,\omega')d\omega' . \quad (2)$$

The first term in Eq. (2) accounts for the density correlations of electrons that dynamically follow the ion motion. This includes both the bound electrons, represented by the ion form factor $f_I(k)$, and the screening cloud of free (and valence) electrons that surround the ion, represented by $q(k)$ [12]. $S_{ii}(k,\omega)$ is the dynamic ion-ion structure factor. The second term in Eq. (2) gives the contribution in the scattering from the free electrons that do not follow the ion motion. Here, $S_{ee}^0(k,\omega)$ is the high frequency part of the electron-electron correlation function [2] and it reduces to the usual electron feature [14] in the case of an optical probe. Inelastic (resonant) scattering by bound electrons is included in the last term of Eq. (2), which arises from bound-free transitions to the continuum of core electrons within an ion, $\tilde{S}_{ce}(k,\omega)$, modulated by the self-motion of the ions, represented by $S_s(k,\omega)$. In Eq. (2), Z is the ionization state and Z_c is the total number of bound (core) electrons per atom.

The calculation of high frequency electron response function as well as the resonant terms have been extensively discussed in the context of WDM and compared with x-ray scattering data from laser produced plasmas [15–17]. The ion acoustic modes in the ion-ion structure factor are separated by $2\hbar\omega_{pi} \sim$ 0.2-1 eV in most WDM states [11], where ω_{pi} is the ion-plasma frequency. This value is considerably smaller than the bandwidth of the laser generated x-ray probe radiation (∼6-20 eV). Accordingly, these modes cannot be resolved with such techniques and it is then reasonable to treat the ionic correlations frequency integrated, that is statically: $S_{ii}(k,\omega) \sim S_{ii}(k)\delta(\omega)$. In view of these limitations, most of the studies so far have concentrated in the evaluation of $S_{ii}(k)$ in WDM under strong coupling conditions with either semi-analytical techniques or by solving the hyper-netted chain (HNC) equations [18, 19].

On the other hand, the advent of 4$^{\text{th}}$ generation light sources such as the FLASH XUV Free Electron Laser (FEL) based in Hamburg and more significantly the hard x-ray sources under commissioning in Stanford (LCLS) and Hamburg (European XFEL), will provide unprecedented ultra-high brillance and coherent pulses for x-ray scattering measurements.

Combining the self-amplified spontaneous emission (SASE) principle of FEL lasing with high harmonic seeding a spectral bandwidth in the order of $\Delta E/E \lesssim 10^{-3}$ can be achieved. With an additional pre-monochromator, it is reasonable to expect $\sim 10^{10}$ photons in a 50-100 fs pulse with bandwidth $\Delta E/E \sim 3 \times 10^{-5}$ or smaller. These machines open up a completely new area of WDM studies where the dynamics of structural phase transitions can be directly investigated by exploiting the full frequency dependence to the ion-ion structure factor $S_{ii}(k, \omega)$.

II. THEORY OF LOW FREQUENCY CHARGE CORRELATIONS

In this paper we will discuss the theoretical framework required to describe the low-frequency ionic fluctuations that enter in the ion-ion structure factor. There exists a couple of approaches to determine the dynamics of the ionic density fluctuations. The usual random phase approximation (RPA) scheme [20] can be extended using static local field corrections [2], the self-consistent STLS approach [21, 22], and the quasi localized charge approximation [23, 24]. The latter works particulary well for very strongly coupled plasmas close to the fluid-solid phase boundary where it showed excellent agreement with molecular dynamics (MD) simulations [25, 26]. However, problems remain for less coupled more fluid ions.

The approach we will follow is based on a memory function [27, 28] description of the ionic correlations. This has the advantage of incorporating the full effects of multi-body correlations beyond the mean field (random phase) approximations by constructing a sequence of phenomenological functions that identically satisfy the frequency moment sum rules. Such techniques have been tested against classical MD and HNC simulations showing good agreement [29]. The memory function approach was also been able to reproduced experimental scattering spectra from weakly coupled plasmas [30].

The charge-charge correlation function is the first step in the description of dynamic response of the WDM state. This relates, by the fluctuation-dissipation theorem, to the microscopic dielectric response of the dense plasma. Since we are interested in the low frequency (ionic) response, we can approximate the charge-charge correlation function as [18]

$$S_{ZZ}(k, \omega) = \left[1 - \frac{q(k)}{Z}\right]^2 S_{ii}(k, \omega). \tag{3}$$

This is equivalent in treating the low frequency response in terms of *quasi*-ions (*i.e.,* bare

ions plus their screening charge) interacting with a polarizable background. Following the approach described by Hansen and McDonald [29], we can rewrite the charge-charge structure factor in terms of an unknown *memory function* $N(k,\omega) = N'(k,\omega) + iN''(k,\omega)$. The charge-charge structure factor can then be expressed in a very general form as

$$S_{ZZ}(k,\omega) = \frac{1}{2\pi} \frac{(kv_t)^2 N'(k,\omega)}{\left[\omega^2 - \omega_0^2 - \omega N''(k,\omega)\right]^2 + \left[\omega N'(k,\omega)\right]^2}, \tag{4}$$

where $v_t = (k_B T_i/M)^{1/2}$ is the ion thermal velocity (M is the ion mass and T_i is the ion temperature, which doesn't need to be equal to the electron temperature), and $N'(k,\omega)$ represents the damping of the plasma waves and $N''(k,\omega)$ their dispersion. Here $\omega_0^2 = \Omega_2/\Omega_0$, where the frequency moments Ω_n are defined as

$$\Omega_n(k) = \int \omega^n S_{ZZ}(k,\omega) d\omega. \tag{5}$$

The phenomenological memory function approach consists in choosing a suitable form for the memory function $N(k,\omega)$ such that as many as possible frequency moments are satisfied.

Conservations laws (particle, current, etc.) can be used to obtain closed expressions of these moments. We notice that since for a classical plasma (which is a reasonably good approximation for the ionic subsystem in WDM states) the charge-charge correlation function is symmetric in frequency, *i.e.*, $S_{ZZ}(k,\omega) = S_{ZZ}(k,-\omega)$, implying that all the odd frequency moments are identically zero. We have for the zeroth moment:

$$\Omega_0 = S_{ZZ}(k) = \left[1 - \frac{q(k)}{Z}\right]^2 S_{ii}(k), \tag{6}$$

where $q(k)$ and $S_{ii}(k)$ are given, for example, by the formulas in Ref. [18], which we will refer to as the screened one-component plasma (SOCP) model. Alternatively, we could use Debye-Hückel (DH) formulas for such terms [31]. In the following section we will compare results from both models. The second moment sum rule (also know as the f-sum rule) is given by [27]

$$\Omega_2 = (kv_t)^2 = \frac{k^2 k_B T_i}{M}, \tag{7}$$

and for the fourth moment [28]

$$\Omega_4 = 3(kv_t)^4 + \left(\frac{\hbar k^2}{2M}\right)^2 (kv_t)^2 + \omega_{pi}^2 (kv_t)^2 \left[1 - I(k)\right], \tag{8}$$

where $\omega_{pi}^2 = Ze^2 n_e/\epsilon_0 M$ (charge neutrality between electron and ions gives $n_e = Zn_i$) and $I(k)$ is the short wavelength limit of the local field correction [28]

$$I(k) = -\frac{Z}{4\pi^2 n_e}\int_0^\infty dq\, q^2\,[S_{ZZ}(q)-1]\times \left[\frac{5}{6}-\frac{q^2}{2k^2}+\frac{(k^2-q^2)^2}{4qk^2}\ln\left|\frac{k+q}{k-q}\right|\right]. \tag{9}$$

In our formalism, the memory functions are chosen such as the correct three lowest order frequency-moment sum rules are exactly reproduced by the charge-charge correlation function. The advantage of such a representation is that we do not need anymore an exact microscopic theory to derive the spectrum of the longitudinal density fluctuations. Conversely, the spectrum is obtained in a form that is phenomenologically self-consistent. Assuming that the memory functions are much simpler objects than the density correlation itself (as confirmed by molecular dynamics simulations), we adopt the following gaussian form for the damping function [29]

$$N'(k,\omega) = \sqrt{\pi}\tau_k(\omega_{1l}^2-\omega_0^2)\exp(-\tau_k^2\omega^2), \tag{10}$$

where $\omega_{1l}^2 = \Omega_4/\Omega_2$ and τ_k is the (k-dependent) relaxation time for the damping of the collective modes. We notice that $\omega = \omega_{1l}$ is the memory function equivalent to the dispersion relation, and it reduces to the usual Bohm and Gross dispersion relation for an ideal and classical plasma [2]. In the case of an electron gas and including local field effects beyond the random phase approximation, this has indeed shown excellent agreement with experimental data on beryllium [8, 32]. From the analytic properties of the response function, and hence of $N(k,\omega)$, the dispersion memory function $N''(k,\omega)$ is then obtained from $N'(k,\omega)$ with the help of the Kramers-Kronig relation [27, 29]

$$N''(k,\omega) = -\mathcal{P}\frac{1}{\pi}\int\frac{N'(k,\omega')}{\omega'-\omega}d\omega' = 2\tau_k(\omega_{1l}^2-\omega_0^2)\exp(-\tau_k^2\omega^2)\int_0^{\tau_k\omega}\exp(y^2)dy, \tag{11}$$

with $\mathcal{P}$ denoting the principal part of the integral. The relaxation time τ_k is related to the sixth moment of the charge-charge correlation function [29]. We have,

$$\tau_k^2 = \frac{\omega_{1l}^2-\omega_0^2}{2(\Omega_6/\Omega_2-\omega_{1l}^4)}. \tag{12}$$

Although explicit expressions for Ω_6 are available [33, 34], they are rather complicated and difficult to evaluate since they involve triplet correlation functions in slowly convergent

integrals [35]. The superposition approximation [34] is often used in the evaluation of the triplet correlation functions.

In order to overcome this problem, we notice that not all the details of the correlation function are required in order to compute the frequency moments. Let us consider a simplified version, $\tilde{S}_{ZZ}(k,\omega)$, of the charge-charge structure factor. In the long wavelength limit, $\tilde{S}_{ZZ}(k,\omega)$ can be written as a sum of ion-acoustic excitations plus single particle excitations [36], thus

$$\tilde{S}_{ZZ}(k,\omega) = S_{ZZ}(k)\left\{\frac{1}{2}A\left[\delta(\omega-\omega_{1l})+\delta(\omega+\omega_{1l})\right]+ (1-A)\frac{1}{\sqrt{\pi}\gamma}\exp(-\omega^2/\gamma^2)\right\}, \tag{13}$$

where $\gamma = 2\omega_{1l}^2/3$ and

$$A = \frac{1}{2}\frac{\omega_0^2-\omega_{1l}^2/3}{\omega_{1l}^2/3}, \tag{14}$$

are chosen such that $\tilde{S}_{ZZ}(k,\omega)$ satisfies all the sum rules up to the fourth frequency moment. This is indeed a very simple approximation and it neglects any damping on the ion modes resulting from triplet correlations, but we believe it is adequate up to moderate ion coupling conditions. We can then use $\tilde{S}_{ZZ}(k,\omega)$ to derive an approximate form for the sixth moment, and we obtain

$$\Omega_6 \approx \frac{1}{3}(kv_t)^2\omega_{1l}^4\left(2+\frac{\omega_{1l}^2}{\omega_0^2}\right). \tag{15}$$

With this equation, the charge-charge dynamic structure factor is fully determined once all the static (frequency integrated) properties have been obtained for a given plasma state. We should note that despite being derived in the long wavelength limit, our expression for Ω_6 reproduces the correct limit for short wavelength. In this case, $\Omega_6(k\to\infty) = 15(kv_t)^6$ as shown in Refs. [33, 34].

III. THE ION-ION STRUCTURE FACTOR

In the memory function description of the charge-charge structure factor we have essentially assumed that the ions behave as classical particles (*i.e.,* we have used the classical form of the sum rules). Since we are dealing with ionic dynamics, it is reasonable to assume that quantum aspects not associated with detailed balance are marginal. This indeed has shown excellent agreement with liquid metal data [37]. On the other hand, quantum

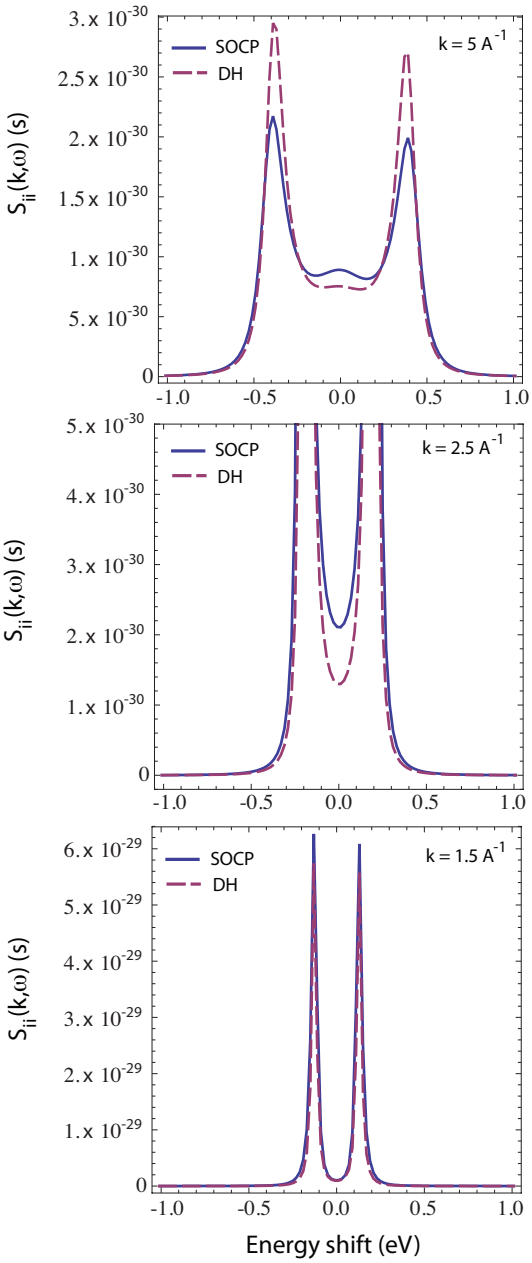

FIG. 1: (Color online) Calculated structure factors $S_{ii}(k)$ for a WDM lithium plasma with $T_i = T_e = 4.5$ eV, $n_e = 7 \times 10^{22}$ cm^{-3}, and $Z = 1.35$. The sharp peaks in the structure factors are unresolved in the calculations. The energy shift corresponds to $\hbar\omega$.

effects directly associated with detailed balance are not always negligible, especially if we are dealing with excitations such as $\hbar\omega_{1l} \approx k_B T_i$. In those cases, we follow the prescription of Ref. [37] of including detailed balance as a multiplicative factor in front of the classical

structure factor, *i.e.,*

$$S_{ZZ}(k,\omega) \to \frac{\hbar\omega/k_B T_i}{1-\exp\left(-\frac{\hbar\omega}{k_B T_i}\right)} S_{ZZ}(k,\omega). \tag{16}$$

Thus by virtue of Eq. (4) we have for the ion-ion structure factor [37]

$$S_{ii}(k,\omega) = \frac{\hbar\omega/k_B T_i}{1-\exp\left(-\frac{\hbar\omega}{k_B T_i}\right)} \left[1-\frac{q(k)}{Z}\right]^{-2} S_{ZZ}(k,\omega), \tag{17}$$

where the first factor includes the effects of detail balance (not associated with particle correlations) and with the charge-charge structure factor obtained from the analysis given in the previous section.

Fig. 1 shows $S_{ii}(k,\omega)$ calculations for conditions expected in a dense lithium plasma [11]. In particular, we have compared results from both the SOCP and the DH models for the static properties. These shows a moderate increase of damping in the SOCP model with respect the ideal case represented by the Debye-Hückel theory. This is expected since multi-body effects (*i.e.,* collisions) will play an important role in enhancing de-correlation on collective modes. Plots of the structure factors (in the SOCP approximation for the static properties) with different plasma temperature are given in Fig. 2. These clearly indicates thermal broadening (Landau damping) of the resonances and the effect of thermal pressure in the dispersion relation (*i.e.,* the position of the resonances). Experiments are indeed required to resolve the details of damping and dispersion, thus providing the necessary tool for the validation of these theoretical models.

We note that in the long wavelength limit, from Eq. (13), the intensity of the ion acoustic resonances for a semi-classical plasma is given by

$$S_{ii}^{\rm peak} \simeq \frac{3k_{De}^6 (ZT_e/T_i)}{4k^6\left[1-I(0)\right]}, \tag{18}$$

where k_{De} is the inverse of the (electron) Debye length. In absence of correlations, $I(0)=0$, and the peak intensity will decrease with increasing ion temperature. Since $I(0)$ is directly related to the compressibility of the system [2], deviations from a monotonic decrease with temperature will be thus associated to non-ideal effects, which in principle, could be measured in a dedicated experiment.

The calculation presented so far in Figs. 1 and 2 have assumed a WDM plasma in thermodynamic equilibrium ($T_e = T_i$). In principle this is not required in our analysis and extensions to non equilibrium systems can be readily performed. As discussed in Ref. [31]

and references therein, the fluctuation-dissipation theorem remains applicable if the temperature relaxation is slow compared to the electron density fluctuation time scale. A common condition in experimental plasmas for this to occur is when the ion mass is much larger than the electron mass, so that the coupling between the two components take place at a sufficiently low frequency.

IV. FEASIBILITY OF FEL EXPERIMENTS

As indicated in both Figs. 1 and 2, the separation between the ion-acoustic resonances is of the order of 0.4-1 eV for a dense lithium plasma. Achieving such a resolution is now possible with the advent of 4$^{\text{th}}$ generation light sources and future high resolution inelastic x-ray scattering experiments could then provide a direct method to test the proposed model of ionic correlation by measuring the position and the broadening of the ionic resonances. The expected bandwidth for the Linear Coherent Light Source (LCLS) under final commissioning at Stanford is $\Delta E/E \sim 0.2\%$ which gives 4 eV for 2 keV probe x-rays in the 1$^{\text{st}}$ harmonic (delivering 10^{12} photons per $\sim$100 fs pulse). This then requires an additional monochromating station to be added in the incident beam path. With a Si (311) double crystal monochromator, a bandwidth $\Delta E/E \sim 3\times10^{-5}$ can be achieved (equivalent to 0.06 eV for 2 keV x-rays). While this is theoretically sufficient for discriminating the peaks in the ion feature, additional broadening mechanisms associated with inhomogeneity in the sample must also be included. These typically arises from temperature and density gradients. As shown by Belyi [38], the effect of macroscopic inhomogeneities introduces an effective broadening of the resonance lines given by

$$\Delta\omega_k \sim \frac{2}{\Lambda_t} + \frac{\omega_{pi}}{k\Lambda_l}\left[1+\frac{6(kv_t)^2}{\omega_{pi}^2}\right], \tag{19}$$

where Λ_t is the characteristic scale length of temporal macroscopic fluctuations (which are in the order of the FEL pulse length), and Λ_l is the characteristic scale length of spatial gradients. The second term usually dominates over the first one. Assuming that the spatial gradients are produced by the propagation of a thermal wave from a femtosecond optical pump laser focussed on the sample, $\Lambda_l \sim \text{few}\times v_t\tau_L$ (where $\tau_L = 100$ fs is the duration of the FEL pulse), we get that for the conditions of this work $\Delta(\hbar\omega_k) < 0.1$ eV. Thus, while some broadening induced by spatial gradients is expected, it will still be possible to resolve the

peak structure in the ion feature, especially for the large k cases. A significant improvement could be achieved if the optical pump laser is replaced by a secondary FEL beam. For a soft x-ray pump, the gradient scale length on a Li sample is several microns, and in this case spatial broadening effects are completely negligible.

Another important parameter that determines the overall feasibility of the experiment is the total photometric efficiency. As discussed above, an inline monochromator is required to achieve the desired bandwidth. This will reduce the total number of photons per shot arriving at the sample to $N_{ph} \sim 10^{10}$. The total number of detected photons per shot is

$$N_d \simeq N_{ph} Z_A^2 n_i \sigma_T L \frac{\Omega_{dect} R_{crystal} \eta_{dect}}{4\pi}, \tag{20}$$

where $Z_A = 3$ is the lithium atomic number, σ_T is the Thomson cross section, L is the sample thickness (which we assume to be 100 μm), Ω_{dect} is the solid angle of the crystal spectrometer used for detection of the scattered x-rays, $R_{crystal}$ is the integrated crystal reflectivity and η_{dect} is the overall efficiency of the CCD detector ($\sim$95% for a back thinned silicon chip). If we assume that the scattered photons are detected with a 50 mm x 50 mm highly annealed pyrolitic graphite (HAPG) crystal [39] placed at a distance 0.5 m in a Von Hamos focussing geometry, $\Omega_{dect} = 0.01$ sr and $R_{crystal} \approx 0.02$, thus $N_d \approx 500$ per shot. If we use a CCD camera that has an analog-to-digital (A/D) gain of $g_{AD} = 3.5$ electron-hole pairs per count and $g_{eh} = 3.6$ eV is the energy required to liberate an electron-hole pair in the silicon, then the number of counts per incident photon of energy $E_{\rm x} = 2$ keV is $E_{\rm x}/g_{AD}g_{eh}$ and the total expected number of counts per shot is $\sim$80000. These will be distributed over about 10 x 10 pixels, giving 800 counts per pixel per shot. This number is significantly higher than the r.m.s. readout noise of a cooled CCD camera and single shot detection is clearly possible.

We should stress that the use of a HAPG crystal is important, but not essential for single shot operations. These crystals can have a narrow rocking curve with high integrated reflectivity. Assuming a mosaic spread $\gamma_m = 0.04^{\rm o}$ [39], the expected resolution is 0.2 eV (source broadening is not important for the suggested configuration, and it only amounts to 0.008 eV), which is sufficient for the detection of the ion acoustic peaks for the larger wavenumber and temperature cases. A significant gain in crystal bandwidth can be obtained if, instead, we use a perfect crystal (*e.g.,* Si), but in this case an improvement by a factor of $\sim$10 in the rocking curve will likely result in a reduction by a similar factor of the expected number of counts per pixel per shot. Again, single shot operation at $\sim$80 counts per pixel

per shot is possible if the r.m.s. noise from any possible source is maintained at a minimum level. However, since LCLS (and XFEL) can run at a repetition rate of 30 Hz, integration over multiple shots is also feasible and, in this case, multiple shot acquisition over a few minutes will then generate enough signal counts for high signal-to-noise ratio data.

V. SUMMARY

We have presented a detailed statistical model for the low frequency ion response based on the phenomenological memory function formalism. This has allowed to construct a closed form expression for the frequency dependent ion-ion structure factor which is applicable in WDM system by fully accounting for strong coupling effects by identically satisfying the sum rules up to the sixth moment. A detailed photometric analysis, both in terms of required bandwidth and photon number at the detector, has shown that experimental measurement of the the ion acoustic peaks will be possible for the proposed 4^{th} generation light sources. We also notice that the blue and red sides of the scattering spectrum are modulated by the detailed balance relation [27]. This implies that such experiments could be used to directly measure the ion temperature *independently* of any assumptions on the correlation functions. If this type of experiment is then combined to the ones already proposed to investigate the plasmon resonances resulting from the high frequency electron correlations [40], then we could envision an experimental platform where both the electron and the ion temperatures are measured simultaneously (and independently) using the detailed balance relation. Clearly this would enable a very powerful tool to look at energy relaxation processes in WDM systems in a pump-probe configuration, thus providing a guidance on current uncertainties in the equilibration process modeling of dense plasmas [41, 42].

Acknowledgements

This work was partially supported by the EPSRC grant EP/G007187/1 and by the Science and Technology Facilities Council of the United Kingdom. GG would like to thank Dr Thomas Tschentscher (European XFEL, Hamburg) for discussions on the hard x-ray FEL

beamlines being planned.

---

[1] National Research Council. *Frontiers in high energy density physics : the x-games of contemporary science* (National Academies Press, Washington, D.C., 2003).

[2] S. Ichimaru, Rev. Mod. Phys. **54**, 1017(1982).

[3] J. Lindl, Phys. Plasmas **2**, 3933 (1995).

[4] T. Guillot, Science **286**, 72 (1999).

[5] M. Koenig, A. Benuzzi-Mounaix, A. Ravasio, T. Vinci, N. Ozaki, S. Lepape, D. Batani, G. Huser, T. Hall, D. Hicks, A. Mackinnon, P. Patel, H. S. Park, T. Boehly, M. Borghesi, S. Kar and L. Romagnani, Plasma Phys. Contr. Fusion **47**, B441 (2005).

[6] J. R. Rygg, F. H. Séguin, C. K. Li, J. A. Frenje, M. J.-E. Manuel, R. D. Petrasso, R. Betti, J. A. Delettrez, O. V. Gotchev, J. P. Krauner, D. D. Meyerhofer, F. J. Marshall, C. Stoeckl and W. Theobald, Science **319**, 1223 (2008).

[7] S. H. Glenzer, G. Gregori, R. W. Lee, F. J. Rogers, S. W. Pollaine and O. L. Landen, Phys. Rev. Lett. **90**, 175002 (2003).

[8] S. H. Glenzer, O. L. Landen, P. Neumayer, R. W. Lee, K. Widmann, S. W. Pollaine, R. J. Wallace, G. Gregori, A. Höll, T. Bornath R. Thiele, V. Schwarz, W.-D. Kraeft and R. Redmer, Phys. Rev. Lett. **98**, 065002 (2007).

[9] A. Ravasio, G. Gregori, A. Benuzzi-Mounaix, J. Daligault, A. Delserieys, A. Ya. Faenov, B. Loupias, N. Ozaki, M. Rabec Le Gloahec, T. A. Pikuz, D. Riley and M. Koenig, Phys. Rev. Lett. **99** 135006 (2007).

[10] G. Gregori, S. H. Glenzer, K. B. Fournier, K. M. Campbell, E. L. Dewald, O. S. Jones, J. H. Hammer, S. B. Hansen, R. J. Wallace and O. L. Landen, Phys. Rev. Lett **101**, 045003 (2008).

[11] E. García Saiz, G. Gregori, D. O. Gericke, J. Vorberger, B. Barbrel, R. J. Clarke, R. R. Freeman, S. H. Glenzer, F. Y. Khattak, M. Koenig, O. L. Landen, D. Neely, P. Neumayer, M. M. Notley, A. Pelka, D. Price, M. Roth, M. Schollmeier, C. Spindloe, R. L. Weber, L. van Woerkom, K. Wünsch and D. Riley, Nature Phys. **4**, 940 (2008).

[12] J. Chihara, J. Phys.: Condens. Matter **12**, 231 (2000).

[13] G. Gregori, S. H. Glenzer, W. Rozmus, R. W. Lee and O. L. Landen, Phys. Rev. E **67**, 026412 (2003).

[14] D.E. Evans and J. Katzenstein, Rep. Prog. Phys. **32**, 207 (1969).

[15] G. Gregori, S. H. Glenzer and O. L. Landen, J. Phys. A: Math. Gen. **36**, 5971 (2003).

[16] A. Höll, R. Redmer, G. Röpke and H. Reinholz, Eur. Phys. J. D **29**, 159 (2004).

[17] S. Sahoo, G. F. Gribakin, G. Shabbir Naz, J. Kohanoff and D. Riley, Phys. Rev. E **77**, 046402 (2008).

[18] G. Gregori, A. Ravasio, A. Höll, S. H. Glenzer and S. J. Rose, High Energy Density Phys. **3**, 99 (2007).

[19] K. Wünsch, P. Hilse, M. Schlanges and D. O. Gericke, Phys. Rev E **77**, 056404 (2008).

[20] D. Pines and D. Bohm, Phys. Rev. **85**, 338 (1952).

[21] K. S. Singwi, M. P. Tosi, R. H. Land and A. Sjolander, Phys. Rev. **176**, 589 (1968).

[22] K. S. Singwi, M. P. Tosi, R. H. Land and A. Sjolander, Solid State Commun. **7** 1503 (1970).

[23] G. Kalman, K. I Golden, Phys Rev A **41**, 5516 (1990).

[24] K. I. Golden, G. Kalman, Phys. Plasmas **7**, 14 (2000).

[25] G. J. Kalman, P. Hartmann, Z. Donkò and M. Rosenberg, Phys. Rev. Lett. **92**, 065001 (2004).

[26] Z. Donkò, G. J. Kalman and K. I. Golden, Phys. Rev. Lett. **88**, 225001 (2002).

[27] J.-P. Hansen and I.R. McDonald, *Theory of Simple Liquids* (Academic, London, 2000).

[28] A. A. Kugler, J. Stat. Phys. **12**, 35 (1975).

[29] J.-P. Hansen, I. R. MacDonald and E. L. Pollock, Phys. Rev. A **11**, 1025 (1975).

[30] G. Gregori, U. Kortshagen, J. Heberlein and E. Pfender, Phys. Rev. E **65**, 046411 (2002).

[31] G. Gregori, S. H. Glenzer and O. L. Landen, Phys. Rev. E **74**, 026402 (2006).

[32] R. Thiele, T. Bornath, C. Fortmann, A. Höll, R. Redmer, H. Reinholz, G. Röpke, A. Wierling, S. H. Glenzer and G. Gregori, Phys. Rev. E **78**, 026411 (2008).

[33] P. Vieillefosse and J.-P. Hansen, Phys. Rev. A **12**, 1106 (1975).

[34] H. B. Singh, Aruna Sharma and K. N. Pathak, Phys. Rev A **19**, 899 (1979).

[35] B. Brami and F. Joly, Physica A **139**, 306 (1986).

[36] S. Ichimaru, H. Totsuji, T. Tange and D. Pines, Progr. Theor. Phys. **54** 1077 (1975).

[37] T. Scopigno, G. Ruocco and F. Sette, Rev. Mod. Phys. **77**, 881 (2005).

[38] V. V. Belyi, Phys. Rev. Lett. **88**, 255001 (2002).

[39] H. Legall, H. Stiel, V. Arkadiev and A. A. Bjeoumikhov, Optics Express **14**, 4570 (2006).

[40] A. Höll, Th. Bornath, L. Cao, T. Döppner, S. Düsterer, E. Föster, C. Fortmann, S. H. Glenzer, G. Gregori, T. Laarmann, K.-H. Meiwes-Broer, A. Przystawik, P. Radcliffe, R. Redmer, H.

Reinholz, G. Röpke, R. Thiele, J. Tiggesbäumker, S. Toleikis, N. X. Truong, T. Tschentscher, I. Ushmann and U. Zastrau, High Energy Density Phys. **3**, 120 (2007).

[41] J. Daligault and D. Mozyrsky, High Energy Density Phys. **4**, 58 (2008).

[42] G. Gregori and D. O. Gericke, Europhys. Lett. **83**, 15002 (2008).

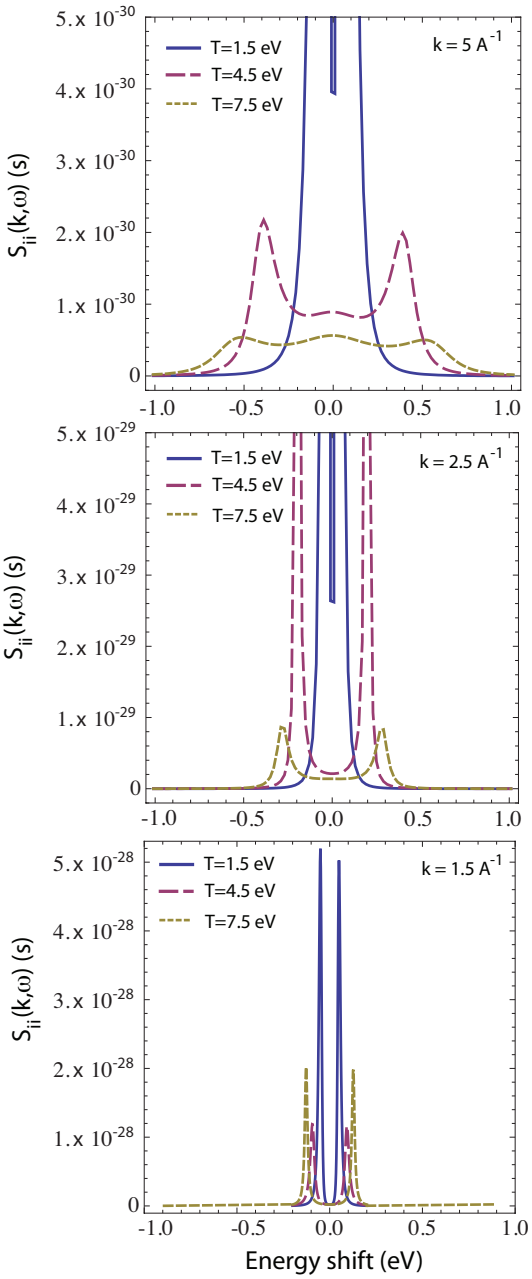

FIG. 2: (Color online) Calculated structure factors $S_{ii}(k)$ for a WDM lithium plasma in thermodynamic equilibrium ($T_e = T_i$) with $n_e = 7 \times 10^{22}$ cm^{-3}, and $Z = 1.35$. Static properties have been obtained from the SOCP model. The sharp peaks in the structure factors are unresolved in the calculations. The energy shift corresponds to $\hbar\omega$.